EH3 (ABHD9): the first member of a new epoxide hydrolase family with high activity for fatty acid epoxides[S]

Martina Decker,[1,]* Magdalena Adamska,[1,]* Annette Cronin,* Francesca Di Giallonardo,*
Julia Burgener,* Anne Marowsky,* John R. Falck,[†] Christophe Morisseau,[§] Bruce D. Hammock,[§]
Artiom Gruzdev,** Darryl C. Zeldin,** and Michael Arand[2,]*

Institute of Pharmacology and Toxicology,* University of Zurich, 8057 Zurich, Switzerland; Southwestern Medical Center,[†] University of Texas, Dallas, TX 75390; Entomology and Comprehensive Cancer Research Center,[§] University of California, Davis, CA 95616; and Division of Intramural Research,** National Institute of Environmental Health Sciences, National Institutes of Health, Research Triangle Park, NC 27709

Abstract **Epoxide hydrolases are a small superfamily of enzymes important for the detoxification of chemically reactive xenobiotic epoxides and for the processing of endogenous epoxides that act as signaling molecules. Here, we report the identification of two human epoxide hydrolases: EH3 and EH4. They share 45% sequence identity, thus representing a new family of mammalian epoxide hydrolases. Quantitative RT-PCR from mouse tissue indicates strongest EH3 expression in lung, skin, and upper gastrointestinal tract. The recombinant enzyme shows a high turnover number with 8,9-, 11,12-, and 14,15-epoxyeicosatrienoic acid (EET), as well as 9,10-epoxyoctadec-11-enoic acid (leukotoxin). It is inhibited by a subclass of N,N'-disubstituted urea derivatives, including 12-(3-adamantan-1-yl-ureido)-dodecanoic acid, 1-cyclohexyl-3-dodecylurea, and 1-(1-acetylpiperidin-4-yl)-3-(4-(trifluoromethoxy)phenyl)urea, compounds so far believed to be selective inhibitors of mammalian soluble epoxide hydrolase (sEH).** **Its sensitivity to this subset of sEH inhibitors may have implications on the pharmacologic profile of these compounds. This is particularly relevant because sEH is a potential drug target, and clinical trials are under way exploring the value of sEH inhibitors in the treatment of hypertension and diabetes type II.**—Decker, M., M. Adamska, A. Cronin, F. Di Giallonardo, J. Burgener, A. Marowsky, J. R. Falck, C. Morisseau, B. D. Hammock, A. Gruzdev, D. C. Zeldin, and M. Arand. **EH3 (ABHD9): the first member of a new epoxide hydrolase family with high activity for fatty acid epoxides.** *J. Lipid Res.* 2012. 53: 2038–2045.

Supplementary key words epoxyeicosatrienoic acid • blood pressure • pain • diabetes type II

Epoxide hydrolases (EH) are enzymes that hydrolyze oxirane (epoxide) derivatives to the corresponding diols. They serve a plethora of vital functions, including detoxification of chemically reactive epoxides (1) and formation of defense barriers by plants against herbivores (2), as well as the regulation of a large variety of physiological functions (3). The latter capability is due to the fact that a growing number of lipid-derived epoxides has been identified as signaling molecules in higher organisms. This is best documented for the arachidonic acid-derived epoxides, in particular, the epoxyeicosatrienoic acid (EET) regioisomers that have been shown to be involved in the regulation of, for example, blood pressure (4, 5), pain perception (6, 7), angiogenesis (8), and inflammation (9). Thus, pharmacologic intervention in the pathways controlling their biologic activity is an appealing target for drug development (10, 11).

The vast majority of EHs belong to the structural family of α/β hydrolase fold enzymes and share the same three-dimensional structure and enzymatic mechanism (12), with few exceptions (13–15). Two mammalian α/β hydrolase fold EHs have been described and studied in detail. The microsomal epoxide hydrolase (mEH) is the major player

in the defense against reactive, xenobiotic-derived epoxides (16). Recent results suggest that it also plays a role in signaling molecule processing (17). The sister enzyme soluble epoxide hydrolase (sEH) (18) serves a prominent function in the processing of important signaling molecules (19, 20), in particular EETs. In addition, it complements the detoxification function of mEH by inactivation of *trans*-disubstituted epoxides (21) that escape the otherwise very broad mEH substrate spectrum.

Like all α/β hydrolase fold enzymes, EHs hydrolyze their substrate via intermediate formation of an enzyme-substrate ester (22, 23). Two structural features in the active site distinguish EHs from the large pool of other α/β hydrolase fold enzymes: *i*) EHs possess an aspartic acid residue as the catalytic nucleophile to form said ester intermediate, and *ii*) they use two tyrosines in their lid domain to recognize and activate the substrate (for details on the enzymatic mechanism, see supplementary data I).

On the basis of such structural characteristics, we have identified three potential new mammalian EHs and describe here the biochemical properties of one of these, namely EH3, in detail. This novel human EH, together with its relative EH4, forms a new family of mammalian EHs and displays a high turnover number with fatty acid-derived epoxides, indicating a role in the regulation of important physiological processes.

MATERIALS AND METHODS

Database screening for candidate epoxide hydrolases

Screening of the "build protein" database on the NCBI Human Genome BLAST website was performed using the BLASTP algorithm with the amino acid sequence RVIAPDLRGYGDSDKP as the search motif. Obtained hits were inspected for the presence of other sequence motifs indicative of an EH function (detailed in supplementary data II).

Cloning and expression of EH3

Human EH3 cDNA was amplified from the IMAGE consortium clone 2226429 (GenBank accession number AI570023). The full-length cDNA was inserted into the pGEF II bacterial expression vector (34). A 5′-truncated cDNA lacking the coding region for the N-terminal 48 amino acid residues was cloned into the bacterial expression vector pRSET B (Invitrogen, Basel, Switzerland) to obtain an anchorless, N-terminally His-tagged fusion protein. The resulting constructs were verified by sequencing and transformed into *E. coli* BL21AI for recombinant expression as described (24). For the expression in insect cells, the full-length cDNA was inserted into the pFastBac plasmid (Invitrogen). Recombination with the baculovirus genome was achieved by transformation of the resulting pFastBac EH3 into *E. coli* DH10Bac. The resulting bacmid was purified, verified by PCR and sequencing, and used to transfect Sf9 insect cells to generate the intact recombinant baculovirus. Recombinant protein expression was accomplished by insect cell infection in suspension culture at a multiplicity of infection of 5. Five days post infection, cells were harvested. Lysates were obtained by a single pass through a FrenchPress pressure cell (American Instrument Exchange, Haverhill, MA) at 30,000 psi and stored at –80°C until use.

EH3 mutants were produced by mutating pFastBac EH3 via the Quikchange™ mutagenesis procedure (Stratagene, La Jolla, CA) and further processing as described above (for details, see supplementary data IV).

Subcellular fractionation and immunoblot analysis

EH3 was purified under denaturing conditions by preparative coomassie blue-SDS gel electrophoresis (25) from inclusion bodies obtained with the pRSET construct and was used to raise antisera in rabbits as described previously (26). The resulting serum has a detection limit of 0.5 ng of recombinant human EH3 per lane by Western blot analysis (27) at a dilution of 1:1000 using colorimetric detection (see below). To assess the subcellular distribution of EH3, insect cell lysates were subjected to differential centrifugation (10,000 *g* for 20 min to pellet larger organelles, followed by 100,000 *g* for 1 h to pellet membrane vesicles). Resulting fractions were analyzed by immunoblotting using the EH3-specific rabbit antiserum (1:1000) and an alkaline phosphatase-conjugated goat anti-rabbit secondary antibody (1:10,000; Sigma, St. Louis, MO), followed by colorimetric detection using NBT/X-phosphate. As a positive control for the distribution of ER membrane vesicles in the above procedure, insect cells infected with a recombinant mEH-coding baculovirus were used.

Enzyme assays

Enzymatic hydrolysis of 9,10-epoxystearic acid was assayed by a TLC-based procedure essentially as previously described (28) using a Cyclone™ Storage Phosphor Scanner (PerkinElmer, Waltham, MA) for quantification of the radiometric signals. Hydrolysis of the different EET regioisomers was quantified in insect cell lysates by LC-MS/MS as described (17). Leukotoxin turnover was assayed under the same experimental conditions using the mass transitions 295.2/171.1 and 313.2/201.1 for the quantification of leukotoxin and leukotoxin diol, respectively. Immunoquantification of EH3 in insect cell lysates is detailed in supplementary data V. For inhibition studies, EH3 lysates or purified human sEH were preincubated for 5 min on ice with EH inhibitors at the indicated concentrations prior to addition of the substrate.

Expression analysis of EH3 in mouse tissues

Tissues for mRNA analyses were taken from 12-week-old C57BL/6 mice. Animals were sacrificed and organs were instantly removed by surgery and snap-frozen in liquid nitrogen until further processing. Total RNA was isolated using RNeasy Mini Kit (Qiagen, Hilden, Germany). cDNA synthesis was performed with the High Capacity cDNA Archive Kit (Applied Biosystems). Primer/probe sets for mouse Ephx3 (Mm01345663_m1) and GADPH (Mm99999915_m1) were purchased from Applied Biosystems. Real-time RT-PCR was run with Maxima qPCR Master Mix (Thermo Scientific) and analyzed using the ABI Prism 7700 thermocycler (Applied Biosystems), and differential expression was calculated using the ΔΔCT method. Primer/probe based expression values were validated by Sybr Green real time RT-PCR (Mouse EPHX3 Primers: 5′-tcccatgtcagtgatccaag-3′ and 5′-tggaagtcagacatagacaacagc-3′).

RESULTS

Sequence similarity search reveals three new human candidate epoxide hydrolases

Previous sequence comparisons of epoxide hydrolase-related α/β hydrolase fold enzymes (22, 29) revealed a highly conserved 16 amino acid sequence motif RVIAPDLRGYGDSDKP, which was used as the bait in database searches for new epoxide hydrolase candidates. This resulted in the identification of three new human proteins, designated ABHD7, ABHD9, and peg1/MEST. Their amino

acid sequences are highly conserved among mammalian species. Further inspection of these sequences proved the presence of all signatures necessary for and compatible with an epoxide hydrolase function (detailed in supplementary data II). Sequence alignment of these proteins with other well-characterized EHs revealed that ABHD7 and ABHD9 are most similar to a recently described set of soluble epoxide hydrolases from *Caenorhabditis elegans* (30), and they represent a new family of mammalian epoxide hydrolases due to a shared sequence identity of 45%. A phylogenetic tree indicating this relationship is shown in **Fig. 1**. On the basis of the results reported below, we proposed to rename the ABHD9 and ABHD7 proteins to EH3 and EH4 and the corresponding genes to EPHX3 and EPHX4, respectively, which was approved by the human genome nomenclature committee, and we use these designations throughout this article (for the rationale behind this nomenclature, see supplementary data III).

EH3 is a functional epoxide hydrolase

We concentrated on the physicochemical and functional characterization of EH3 (ABHD9). The human gene has the chromosomal localization 19p13.12 and is transcribed into a 1.8 kb mRNA composed of 7 exons. The respective mRNA codes for a 360 amino acid protein with a predicted molecular weight and isoelectric point of 40,909 Da and pI 7.7, respectively. Residues 22 to 44 are exclusively hydrophobic in nature and are predicted to represent a membrane insertion signal. They are followed by a stretch of arginine residues, which potentially acts as a stop transfer signal, suggesting a cytoplasmic orientation of the protein similar to that reported for mEH (31).

To investigate whether EH3 has the predicted catalytic function, we recombinantly expressed the protein in *E. coli*. We failed to obtain detectable amounts when trying to

express the complete protein. Instead, an N-terminally truncated version of EH3 carrying an N-terminal His-tag was found in appreciable amounts. The recombinant protein was obtained as inclusion bodies and was therefore not useful for the analysis of enzymatic properties. We used it for rabbit immunization after purification and obtained an antiserum that was suitable for the detection of the protein by immunoblotting. Likewise, an attempt to obtain an enzymatically active EH3 via recombinant expression in yeast failed.

The recombinant full-length enzyme was eventually obtained by baculovirus-mediated expression in insect cells. The yield of EH3 protein was low, routinely amounting to around 0.1% of the total cellular protein, as proven by immunoblot analysis. In line with our prediction, the recombinant protein was membrane-bound as demonstrated by the enrichment in the 100,000 *g* pellet of the insect cell homogenate after differential centrifugation (**Fig. 2**).

The insect cell homogenate was used to assess the catalytic capabilities of the recombinant enzyme. Neither styrene 7,8-oxide, a generic substrate that is hydrolyzed by most EHs (32), nor cholesterol 5,6-epoxide, a substrate for a membrane-bound human EH of which the identification has been reported during the preparation of this article (33), was converted to the corresponding diol by EH3. In contrast, we did detect a high turnover of 9,10-epoxystearic acid with the recombinant cell lysate, an enzymatic activity that was essentially absent from mock-infected insect cell lysates.

Now capable of assessing the functional integrity of the enzyme, we tried to solubilize it from the membrane to attempt its purification. However, multiple trials with different types of detergents and a variety of different experimental conditions did not lead to the release of detectable amount of catalytic activity into the 100,000 *g* supernatant. Therefore, we are, at present, not able to obtain the enzyme in a purified, catalytically active form.

D173, Y220, Y281, D307, and H337 are the residues involved in EH3-mediated catalysis

Sequence comparisons (see the figure in supplementary data II) suggested D173 as the catalytic nucleophile and H337-D307 as the charge relay system of the EH3 catalytic triad. Y281 and Y220 were the predicted candidates for the catalytic tyrosines in the lid domain of the enzyme. Y280 was considered as a possible alternative because of its proximity to the neighboring Y281. In line with this, the respective mutants D173A, Y220F, Y281F, D307A, D307N, H337Q, and H337A expressed in insect cells lacked any detectable hydrolytic activity with 9,10-epoxystearic acid (**Fig. 3A**), substantiating the importance of the five modified residues in substrate turnover (Fig. 3B). In contrast, the mutant Y280F displayed significant enzymatic activity, supporting that Y281 is the catalytic tyrosine and showing the lack of substantial effect of a single amino acid exchange when the respective residue is not directly involved in catalysis. In apparent contradiction to our working hypothesis, the mutant D173N showed a substrate turnover similar to that of the Y280F mutant. However, this is compatible
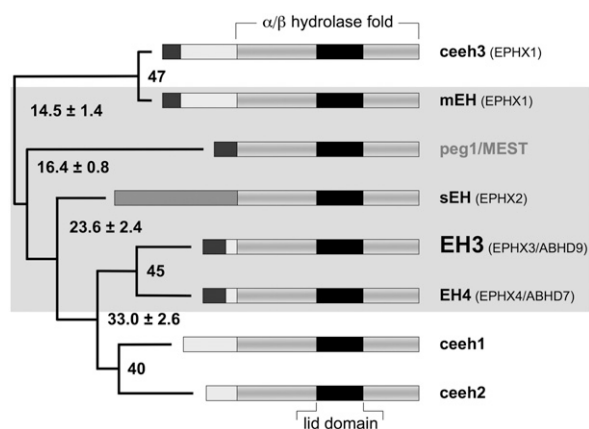
Fig. 1. Phylogenetic tree of epoxide hydrolases. Boxes represent the linear amino acid sequence of human EHs (inside the gray rectangle) compared with their *C. elegans* counterparts. The location of the α/β hydrolase fold domain (gray shaded boxes) and the lid domain (black box) is indicated. Dark gray boxes represent (potential) N-terminal membrane anchor sequences. Sequence alignment was performed using ClustalW (46). The resulting dendrogram on the left side indicates the phylogenetic relation. Numbers at the bifurcations indicate sequence identity (mean sequence identity ± SD, in the case of multiple comparisons).

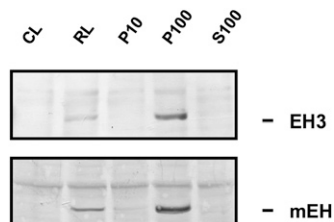**Fig. 2.** Subcellular localization of EH3. Lysates of Sf9 cells expressing human EH3 or rat mEH, used as a microsomal marker, were subjected to differential centrifugation and subsequent immunoblot analysis. Immunoreactivity for EH3 and mEH is restricted to the 100,000 *g* pellet, indicating their membrane association. CL, control insect cell lysate; P10, 10,000 *g* pellet; P100, 100,000 *g* pellet; RL, recombinant insect cell lysate; S100, 100,000 *g* supernatant.

with the expected role of D173 as the catalytic nucleophile because self-activation by autocatalytic hydrolysis from the mutant asparagine to the wild-type aspartic acid side chain has been reported for the equivalent mutants of other EHs (34, 35).

EH3 expression is highest in mouse skin, lung, and upper gastrointestinal tract

To assess the expression pattern of the EH3, we isolated mRNA from a representative set of mouse organs and analyzed these by quantitative RT-PCR (**Fig. 4**). The strongest signals for EH3 expression were obtained with RNA from skin, lung, tongue, esophagus, and stomach. Intermediate expression was found in pancreas and eye, followed by visceral fat, lymph nodes, spleen, aortic arch (used for normalization), and heart. Low signals were obtained with RNA from kidney, testis, ovary intestine, brain, and liver. The lowest detectable expression was found in skeletal muscle.

Epoxyeicosatrienoic acids and leukotoxin are endogenous substrates of EH3

The turnover of 9,10-epoxystearic acid raised the question whether other fatty acid-derived compounds can be hydrolyzed by EH3. We therefore looked at the turnover of EETs and leukotoxin as physiologically relevant substrate candidates. Indeed, EH3 efficiently hydrolyzed all these compounds. **Fig. 5** shows the respective kinetic
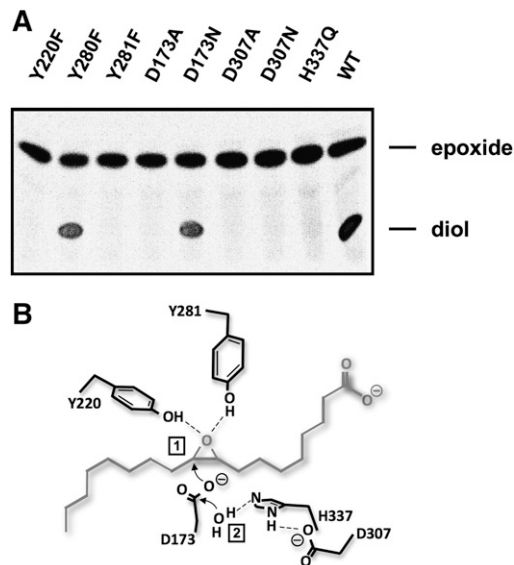

Fig. 3. A: Enzymatic activity analysis of EH3 mutants. Hydrolysis of 9,10-epoxystearic acid by the different mutants was assayed using thin layer chromatography for the separation of substrate (epoxide) and product (diol) of the enzymatic reaction. Identity of the respective mutant is given above each lane. Of all mutants analyzed, only Y280F and D173N displayed enzymatic activity. B: EH3 active site architecture, deduced from the structural alignments and mutant analyses (for details on the enzymatic mechanism, see supplementary data I).

analysis. The derived kinetic constants are given in **Table 1**, in comparison with data obtained with recombinant purified human sEH and mEH under the same conditions. All analyzed substrates were turned over by EH3 with high V_{max}, yet also comparatively high K_m, resulting in catalytic efficacies that are in the range of those obtained with sEH and mEH. The highest catalytic efficacy was observed with leukotoxin. Turnover of 5,6-EET could not be quantified because the insect cell preparation displayed significant background activity with this substrate.

EH3 is inhibited by urea derivatives regarded as specific for sEH

Because EET turnover by EH is evolving as a promising target for therapeutic intervention (11) and, in particular,

A = skin
B = lung
C = tongue
D = esophagus
E = stomach
F = pancreas
G = small intestine
H = large intestine
I = liver
J = kidney
K = heart
L = aortic arch
M = lymph node
N = spleen
O = brain
P = eye
Q = skeletal muscle
R = visceral fat
S = ovary
T = testis

Fig. 4. Expression pattern of EH3 gene in mouse tissues. mRNA isolated from different mouse organs was analyzed by quantitative reverse transcriptase-PCR using EH3-specific primers. Amplification of GAPDH mRNA served as the control. Expression levels in the individual tissues were normalized to those in the aortic arch. The bars represent the average obtained from four individual isolates; error bars indicate SD. The insert shows a magnification of the results obtained from tissues with lower expression yields.
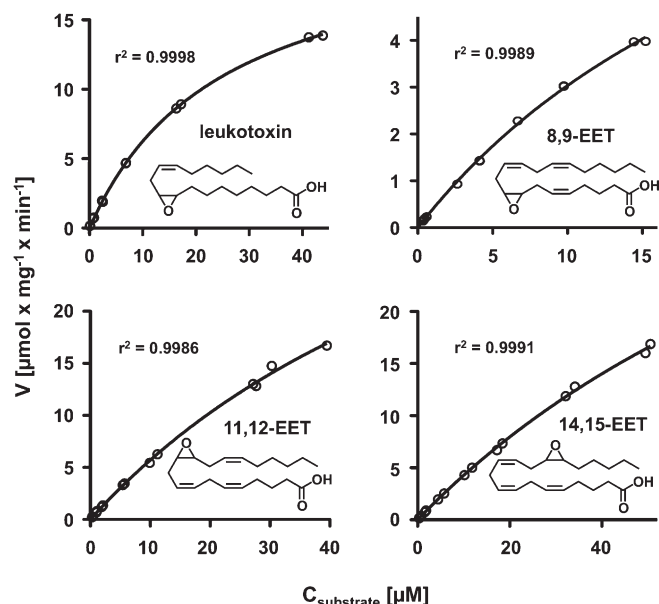
Fig. 5. Kinetic analysis of EH3-catalyzed leukotoxin and EET turnover. Sf9 cell lysates expressing recombinant EH3 were analyzed for the hydrolysis of leukotoxin, 8,-EET, 11,12-EET, and 14,15-EET using substrate concentrations up to 50 μM, depending on the compound. Larger concentrations displayed significant deviations from the Michaelis-Menten kinetic, presumably due to micelle formation of the substrate. Modeling of the Michaelis-Menten kinetic (solid line) was performed using Prism 5 (GraphPad Software, San Diego, CA).

because inhibitors of sEH are being developed as potentially marketable drugs (10), we were interested in a possible interference of such drugs with the EH3-mediated turnover of signaling molecules. We tested a subset of representative EH inhibitors for their inhibitory potency on EH3 catalysis at relevant concentrations (**Table 2**). The classic nonsubstrate inhibitors for mEH (elaidamide) and sEH (ACU) did not affect EH3 activity. Likewise, a new generation of water-soluble sEH inhibitors with bulky structure, represented by 4-(((1*R*,4*R*)-4-(3-(4-(trifluoromethoxy)phenyl)ureido)cyclohexyl)oxy)benzoic acid (t-TAUCB), 4-(((1*S*,4*S*)-4-(3-

((3*S*,5*S*,7*S*)-adamantan-1-yl)ureido)cyclohexyl)oxy)benzoic acid (c-AUCB), and 4-(((1*R*,4*R*)-4-(3-((3*S*,5*S*,7*S*)-adamantan-1-yl)ureido)cyclohexyl)oxy)benzoic acid (t-AUCB), did not show any effect. However, a group of inhibitors hitherto believed to selectively target sEH activity reduced EH3 hydrolysis of 8,9-EET significantly at a concentration of 1 μM. The most potent of these were 1-(1-acetylpiperidin-4-yl)-3-(4-(trifluoromethoxy)phenyl)urea (TPAU), 1-cyclohexyl-3-dodecylurea (CDU) and 12-(3-adamantan-1-yl-ureido)-dodecanoic acid (AUDA), popular sEH inhibitors widely used for in vivo animal studies. We studied their inhibitory profile for EH3 in more detail and determined their IC_{50} (which is expected to equal K_i under the employed experimental conditions) to around 100 nM (**Fig. 6**), thus well in the range to have the enzyme affected under the experimental conditions usually employed for in vivo sEH inhibition (36).

DISCUSSION

EH3 is a hitherto undiscovered mammalian epoxide hydrolase displaying a high turnover with fatty acid-derived epoxides, in particular EETs and leukotoxin, while being essentially inactive toward the generic EH substrate styrene oxide. This substrate selectivity suggests that the enzyme is implicated in processing of signaling molecules rather than detoxification of xenobiotic epoxides. It has the highest specific activity with EETs so far reported for an EH and a catalytic efficacy in the range of that of sEH, the major enzyme in EET turnover (20). Its expression pattern in the mammalian organism is quite different from that of the other well-characterized EHs in that it is poorly expressed in the liver but well expressed in skin, lung, and upper gastrointestinal tract. Based on this observation, it is tempting to speculate on a potential role of EH3 in barrier formation, because the above tissues represent the major contact surfaces with the outside. Indeed, EH3 has been identified as a candidate disease gene for ichthyosis based on comparative studies in human and mouse (37), which is compatible with such a function.

TABLE 1. Catalytic properties of EH3 compared with sEH and mEH

	EH3	sEH	mEH
8,9-EET			
V_{max} [μmol × mg^{-1} × min^{-1}]	12 ± 1	0.9 ± 0.1	0.12 ± 0.1
K_m [μM]	30 ± 3	1.7 ± 0.5	0.8 ± 0.25
k_{cat}/K_m [s^{-1} × M^{-1}]	0.25 × 10^6	0.5 × 10^6	0.12 × 10^6
11,12-EET			
V_{max} [μmol × mg^{-1} × min^{-1}]	50 ± 5	4.5 ± 0.1	0.6 ± 0.03
K_m [μM]	80 ± 10	3.4 ± 0.3	0.4 ± 0.08
k_{cat}/K_m [s^{-1} × M^{-1}]	0.4 × 10^6	1.4 × 10^6	1.2 × 10^6
14,15-EET			
V_{max} [μmol × mg^{-1} × min^{-1}]	60 ± 5	7 ± 0.3	0.04 ± 0.002
K_m [μM]	130 ± 10	15 ± 4	0.9 ± 0.1
k_{cat}/K_m [s^{-1} × M^{-1}]	0.3 × 10^6	0.5 × 10^6	0.03 × 10^6
Leukotoxin			
V_{max} [μmol × mg^{-1} × min^{-1}]	22 ± 0.5	0.55 ± 0.12	0.008 ± 0.0002
K_m [μM]	25 ± 0.6	1.5 ± 0.5	5.8 ± 0.2
k_{cat}/K_m [s^{-1} × M^{-1}]	0.6 × 10^6	0.4 × 10^6	0.001 × 10^6

Data for V_{max} and K_m are given as mean ± SD and represent the average of three to five independent determinations. k_{cat}/K_m is calculated from the means of V_{max} and K_m.

TABLE 2. Inhibition of EH3 catalysis by prototypic EH inhibitors

Inhibitor [1 µM]	EH3	sEH
	Residual Activity (% of Solvent Control ± SD)	
TPAU	7.2 ± 1.4**	2.2 ± 0.7**
AUDA	5.5 ± 0.1**	1.6 ± 0.5**
CDU	7.5 ± 1.2**	2.0 ± 0.3**
AEPU	18 ± 0.7**	4.0 ± 1.5**
AUOA	38 ± 3.9**	14 ± 2.6**
t-TAUCB	97 ± 3.3	0.8 ± 0.1**
c-AUCB	97 ± 4.6	0.2 ± 0.1**
t-AUCB)	99 ± 18	1.2 ± 0.2**
ACU	103 ± 10	8.1 ± 2.2**
Elaidamide	75 ± 6.0	130 ± 3.4*

The molecular structures of the inhibitors are available in supplementary data VI. Data are presented as mean ± SD (n = 3), compared with vehicle control. *$P < 0.05$; **$P < 0.01$.

Furthermore, we found EH3 to be the most efficient catalyst for the hydrolysis of leukotoxin. The resulting metabolite has been reported to be a strong mediator of acute respiratory distress syndrome (ARDS) (19), which suggests that EH3 might contribute to leukotoxin toxicity, in particular as we found a particularly high EH3 expression in the mouse lung (see Fig. 4).

Intriguingly, EH3 is sensitive to inhibition by N,N'-disubstituted urea derivatives, a class of compounds that has been developed as selective inhibitors for the mammalian sEH (38). In contrast to the latter enzyme, EH3 seems to be inhibited only by a subset of these compounds.
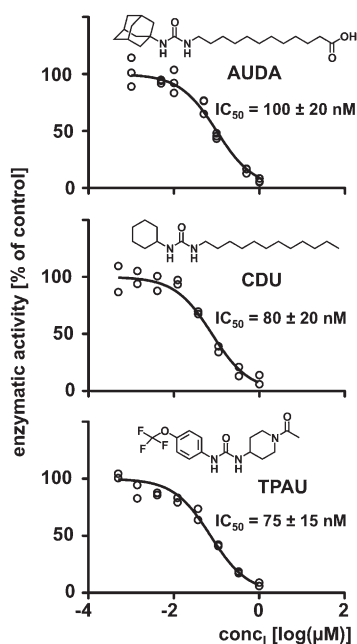
Urea derivatives have been developed as EH inhibitors with the aim to pharmacologically interfere with the EET metabolism and have been proposed as potentially useful agents to treat high blood pressure (10), pain (7), and recently, diabetes type II (39). Our present observation divides the urea derivatives into sEH-selective inhibitors and mixed sEH and EH3 inhibitors. This has to be taken into account for the interpretation of in vivo data obtained with the different sets of compounds. Whether sEH-selective or the mixed-type blockade of EET hydrolysis is more favorable in the treatment of diseases remains to be established.

The expression of the EPHX3 gene has been reported to be downregulated in a variety of tumors. Hypermethylation in the promoter region, associated with a reduced transcription rate, was observed in gastric cancer (40), prostate cancer (41), and melanoma (42). In view of the recently described potential of EETs to reactivate dormant tumors and foster metastasis (43), possibly related to the angiogenic properties of EETs (44), this suggests a potential role of EH3 in the prevention of malignancies.

Finally, it is reasonable to speculate about why there are (at least) three separate EHs for the breakdown of bioactive fatty acid epoxides, namely EH3, sEH, and mEH. Apart from the simple explanation that these differ somewhat in their substrate selectivity, there is an additional intriguing hypothesis: if we accept that the hydrolysis products, like the DHETs and the leukotoxin diol, have

Fig. 6. Determination of IC$_{50}$ (≈ K_i) of AUDA, CDU, and TPAU. EH3 lysate was incubated with either of the three strongest inhibitors identified by the preliminary screening (see Table 2) for 5 min one ice prior to addition of 8,9-EET (5 µM) and analysis of turnover. The enzymatic activity is expressed as percentage of activity of the accompanying solvent control (no inhibitor). Kinetics were modeled using Prism 5. Note that under the present conditions (substrate concentration 7-fold below K_m), the IC$_{50}$ essentially equals K_i (K_i > 90% of IC$_{50}$).
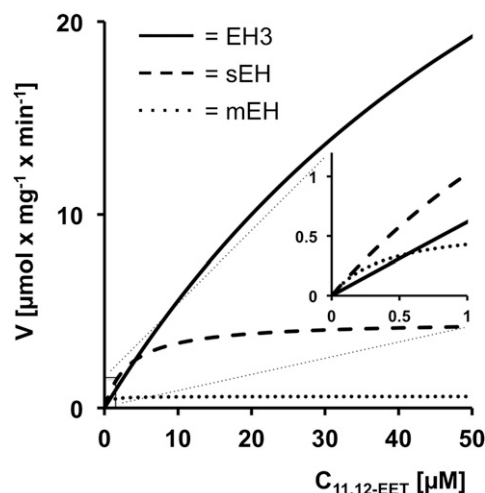

Fig. 7. Comparison of the 11,12-EET turnover kinetics of EH3, sEH, and mEH. The substrate concentration-dependent reaction velocity for equal amounts of each enzyme is displayed. The calculation is based on the experimental data given in Table 1. Although V_{max} dictates the reaction velocity at high substrate concentrations, in the concentration range far below substrate saturation (see inset), the catalytic efficacy is the important predictor. Consequently, the ratio of product formed during hydrolysis versus the substrate concentration is quite similar for all three enzymes at very low substrate concentrations and remains essentially constant with EH3 over the broad range displayed in the graph, whereas it rapidly decreases with increasing substrate concentration in the case of mEH. The sEH displays an intermediate behavior. The potential implications of these differences are discussed in the text.

their own biologic activity as has been reported (19, 45), sometimes distinct and possibly opposite to the effects elicited by the parent molecules, the local ratios in the concentration of epoxide to diol may dictate the signaling outcome. Among the several factors that influence this ratio, the above enzymes particularly differ in two of them, subcellular localization and K_m. The effect of the subcellular localization is obvious. The ER-resident EHs may have a significant kinetic advantage being located in the same subcellular compartment as the epoxide-forming monooxygenase because they might directly hydrolyze the epoxide during their formation, yielding a high diol to epoxide ratio (at least at low epoxide formation rates), as already discussed earlier for mEH (17). The major difference between mEH and EH3, the two ER-resident EHs, is the enormous difference in their K_m for fatty acid epoxides, while their catalytic efficacies are within the same range (see Table 1). The resulting consequences are best explained by looking at a kinetic diagram of the enzymes with a common substrate, 11,12-EET (**Fig. 7**). While both enzymes should afford a similar diol to epoxide ratio at low epoxide formation rates, this ratio would strongly decrease with mEH once the substrate concentration increases over the low mEH K_m, while the ratio would stay constant with EH3 due to its extremely high K_m that lies even beyond the highest locally expected substrate concentration. Thus, EH3 would be the most suitable EH under conditions where a high diol formation rate with only small EET leakage is desired.▪

REFERENCES

1. Oesch, F. 1973. Mammalian epoxide hydrases - inducible enzymes catalyzing inactivation of carcinogenic and cytotoxic metabolites derived from aromatic and olefinic compounds. *Xenobiotica.* **3:** 305–340.
2. Blee, E. 1998. Biosynthesis of phytooxylipins: the peroxygenase pathway. *Lipid/Fett.* **100:** 121–127.
3. Spector, A. A., and A. W. Norris. 2007. Action of epoxyeicosatrienoic acids on cellular function. *Am. J. Physiol. Cell Physiol.* **292:** C996–C1012.
4. Campbell, W. B., D. Gebremedhin, P. F. Pratt, and D. R. Harder. 1996. Identification of epoxyeicosatrienoic acids as endothelium-derived hyperpolarizing factors. *Circ. Res.* **78:** 415–423.
5. Lee, C. R., J. D. Imig, M. L. Edin, J. Foley, L. M. DeGraff, J. A. Bradbury, J. P. Graves, F. B. Lih, J. Clark, P. Myers, et al. 2010. Endothelial expression of human cytochrome P450 epoxygenases lowers blood pressure and attenuates hypertension-induced renal injury in mice. *FASEB J.* **24:** 3770–3781.
6. Conroy, J. L., C. Fang, J. Gu, S. O. Zeitlin, W. Yang, J. Yang, M. A. VanAlstine, J. W. Nalwalk, P. J. Albrecht, J. E. Mazurkiewicz, et al. 2010. Opioids activate brain analgesic circuits through cytochrome P450/epoxygenase signaling. *Nat. Neurosci.* **13:** 284–286.
7. Inceoglu, B., S. L. Jinks, A. Ulu, C. M. Hegedus, K. Georgi, K. R. Schmelzer, K. Wagner, P. D. Jones, C. Morisseau, and B. D. Hammock. 2008. Soluble epoxide hydrolase and epoxyeicosatrienoic acids modulate two distinct analgesic pathways. *Proc. Natl. Acad. Sci. USA.* **105:** 18901–18906.
8. Medhora, M., J. Daniels, K. Mundey, B. Fisslthaler, R. Busse, E. R. Jacobs, and D. R. Harder. 2003. Epoxygenase-driven angiogenesis
9. Smith, K. R., K. E. Pinkerton, T. Watanabe, T. L. Pedersen, S. J. Ma, and B. D. Hammock. 2005. Attenuation of tobacco smoke-induced lung inflammation by treatment with a soluble epoxide hydrolase inhibitor. *Proc. Natl. Acad. Sci. USA.* **102:** 2186–2191.
10. Imig, J. D., and B. D. Hammock. 2009. Soluble epoxide hydrolase as a therapeutic target for cardiovascular diseases. *Nat. Rev. Drug Discov.* **8:** 794–805.
11. Marino, J. P., Jr. 2009. Soluble epoxide hydrolase, a target with multiple opportunities for cardiovascular drug discovery. *Curr. Top. Med. Chem.* **9:** 452–463.
12. Arand, M., A. Cronin, F. Oesch, S. L. Mowbray, and T. A. Jones. 2003. The telltale structures of epoxide hydrolases. *Drug Metab. Rev.* **35:** 365–383.
13. Arand, M., B. M. Hallberg, J. Y. Zou, T. Bergfors, F. Oesch, M. J. van der Werf, J. A. M. de Bont, T. A. Jones, and S. L. Mowbray. 2003. Structure of Rhodococcus erythropolis limonene-1,2-epoxide hydrolase reveals a novel active site. *EMBO J.* **22:** 2583–2592.
14. Fillgrove, K. L., S. Pakhomova, M. R. Schaab, M. E. Newcomer, and R. N. Armstrong. 2007. Structure and mechanism of the genomically encoded fosfomycin resistance protein, FosX, from Listeria monocytogenes. *Biochemistry.* **46:** 8110–8120.
15. Thunnissen, M. M. G. M., P. Nordlund, and J. Z. Haeggstrom. 2001. Crystal structure of human leukotriene A(4) hydrolase, a bifunctional enzyme in inflammation. *Nat. Struct. Biol.* **8:** 131–135.
16. Oesch, F. 1974. Purification and specificity of a human microsomal epoxide hydratase. *Biochem. J.* **139:** 77–88.
17. Marowsky, A., J. Burgener, J. R. Falck, J. M. Fritschy, and M. Arand. 2009. Distribution of soluble and microsomal epoxide hydrolase in the mouse brain and its contribution to cerebral epoxyeicosatrienoic acid metabolism. *Neuroscience.* **163:** 646–661.
18. Hammock, B. D., S. S. Gill, V. Stamoudis, and L. I. Gilbert. 1976. Soluble mammalian epoxide hydratase - action on juvenile hormone and other terpenoid epoxides *Comp. Biochem. Physiol. B.* **53:** 263–265.
19. Moghaddam, M. F., D. F. Grant, J. M. Cheek, J. F. Greene, K. C. Williamson, and B. D. Hammock. 1997. Bioactivation of leukotoxins to their toxic diols by epoxide hydrolase. *Nat. Med.* **3:** 562–566.
20. Zeldin, D. C., J. Kobayashi, J. R. Falck, B. S. Winder, B. D. Hammock, J. R. Snapper, and J. H. Capdevila. 1993. Regiofacial and enantiofacial selectivity of epoxyeicosatrienoic acid hydration by cytosolic epoxide hydrolase. *J. Biol. Chem.* **268:** 6402–6407.
21. Krämer, A., H. Frank, F. Setiabudi, F. Oesch, and H. Glatt. 1991. Influence of the level of cytosolic epoxide hydrolase on the induction of sister chromatid exchanges by *trans*-beta-ethylstyrene 7,8-oxide in human lymphocytes. *Biochem. Pharmacol.* **42:** 2147–2152.
22. Arand, M., D. F. Grant, J. K. Beetham, T. Friedberg, F. Oesch, and B. D. Hammock. 1994. Sequence similarity of mammalian epoxide hydrolases to the bacterial haloalkane dehalogenase and other related proteins - implication for the potential catalytic mechanism of enzymatic epoxide hydrolysis. *FEBS Lett.* **338:** 251–256.
23. Hammock, B. D., F. Pinot, J. K. Beetham, D. F. Grant, M. E. Arand, and F. Oesch. 1994. Isolation of a putative hydroxyacyl enzyme intermediate of an epoxide hydrolase. *Biochem. Biophys. Res. Commun.* **198:** 850–856.
24. Cronin, A., S. Mowbray, H. Durk, S. Homburg, I. Fleming, B. Fisslthaler, F. Oesch, and M. Arand. 2003. The N-terminal domain of mammalian soluble epoxide hydrolase is a phosphatase. *Proc. Natl. Acad. Sci. USA.* **100:** 1552–1557.
25. Schägger, H., H. Aquila, and G. Von Jagow. 1988. Coomassie blue-sodium dodecyl sulfate-polyacrylamide gel electrophoresis for direct visualization of polypeptides during electrophoresis. *Anal. Biochem.* **173:** 201–205.
26. Friedberg, T., W. Kissel, M. Arand, and F. Oesch. 1991. Production of site-specific P450 antibodies using recombinant fusion proteins as antigens. *Methods Enzymol.* **206:** 193–201.
27. Burnette, W. N. 1981. "Western blotting": electrophoretic transfer of proteins from sodium dodecyl sulfate-polyacrylamide gels to unmodified nitrocellulose and radiographic detection with antibody and radioiodinated protein. *Anal. Biochem.* **112:** 195–203.
28. Müller, F., M. Arand, H. Frank, A. Seidel, W. Hinz, L. Winkler, K. Hänel, E. Blee, J. K. Beetham, B. D. Hammock, et al. 1997. Visualization of a covalent intermediate between microsomal epoxide hydrolase, but not cholesterol epoxide hydrolase, and their substrates. *Eur. J. Biochem.* **245:** 490–496.

29. Arand, M., W. Hinz, F. Müller, K. Hänel, L. Winkler, A. Mecky, M. Knehr, H. Dürk, H. Wagner, M. Ringhoffer, et al. 1996. Structure and mechanism of soluble epoxide hydrolase and its relation to microsomal epoxide hydrolase. *In* Control Mechanisms of Carcinogenesis. J. G. Hengstler and F. Oesch, editors. Mainz, Germany. 116–134.

30. Harris, T. R., P. A. Aronov, P. D. Jones, H. Tanaka, M. Arand, and B. D. Hammock. 2008. Identification of two epoxide hydrolases in Caenorhabditis elegans that metabolize mammalian lipid signaling molecules. *Arch. Biochem. Biophys.* **472:** 139–149.

31. Holler, R., M. Arand, A. Mecky, F. Oesch, and T. Friedberg. 1997. The membrane anchor of microsomal epoxide hydrolase from human, rat and rabbit displays an unexpected membrane topology. *Biochem. Biophys. Res. Commun.* **236:** 754–759.

32. Arand, M., A. Cronin, M. Adamska, and F. Oesch. 2005. Epoxide hydrolases: structure, function, mechanism, and assay. *Methods Enzymol.* **400:** 569–588.

33. de Medina, P., M. R. Paillasse, G. Segala, M. Poirot, and S. Silvente-Poirot. 2010. Identification and pharmacological characterization of cholesterol-5,6-epoxide hydrolase as a target for tamoxifen and AEBS ligands. *Proc. Natl. Acad. Sci. USA.* **107:** 13520–13525.

34. Arand, M., H. Hemmer, H. Durk, J. Baratti, A. Archelas, R. Furstoss, and F. Oesch. 1999. Cloning and molecular characterization of a soluble epoxide hydrolase from Aspergillus niger that is related to mammalian microsomal epoxide hydrolase. *Biochem. J.* **344:** 273–280.

35. Pinot, F., D. F. Grant, J. K. Beetham, A. G. Parker, B. Borhan, S. Landt, A. D. Jones, and B. D. Hammock. 1995. Molecular and biochemical evidence for the involvement of the Asp-333-His-523 pair in catalytic mechanism of soluble epoxide hydrolase. *J. Biol. Chem.* **270:** 7968–7974.

36. Parrish, A. R., G. Chen, R. C. Burghardt, T. Watanabe, C. Morisseau, and B. D. Hammock. 2009. Attenuation of cisplatin nephrotoxicity by inhibition of soluble epoxide hydrolase. *Cell Biol. Toxicol.* **25:** 217–225.

37. Ala, U., R. M. Piro, E. Grassi, C. Damasco, L. Silengo, M. Oti, P. Provero, and F. Di Cunto. 2008. Prediction of human disease genes by human-mouse conserved coexpression analysis. *PLOS Comput. Biol.* **4:** e1000043.

38. Morisseau, C., M. H. Goodrow, D. Dowdy, J. Zheng, J. F. Greene, J. R. Sanborn, and B. D. Hammock. 1999. Potent urea and carbamate inhibitors of soluble epoxide hydrolases. *Proc. Natl. Acad. Sci. USA.* **96:** 8849–8854.

39. De Taeye, B. M., C. Morisseau, J. Coyle, J. W. Covington, A. Luria, J. Yang, S. B. Murphy, D. B. Friedman, B. B. Hammock, and D. E. Vaughan. 2010. Expression and regulation of soluble epoxide hydrolase in adipose tissue. *Obesity (Silver Spring).* **18:** 489–498.

40. Yamashita, S., Y. Tsujino, K. Moriguchi, M. Tatematsu, and T. Ushijima. 2006. Chemical genomic screening for methylation-silenced genes in gastric cancer cell lines using 5-aza-2'-deoxycytidine treatment and oligonucleotide microarray. *Cancer Sci.* **97:** 64–71.

41. Cottrell, S., K. Jung, G. Kristiansen, E. Eltze, A. Semjonow, M. Ittmann, A. Hartmann, T. Stamey, C. Haefliger, and G. Weiss. 2007. Discovery and validation of 3 novel DNA methylation markers of prostate cancer prognosis. *J. Urol.* **177:** 1753–1758.

42. Furuta, J., Y. Nobeyama, Y. Umebayashi, F. Otsuka, K. Kikuchi, and T. Ushijima. 2006. Silencing of peroxiredoxin 2 and aberrant methylation of 33 CpG islands in putative promoter regions in human malignant melanomas. *Cancer Res.* **66:** 6080–6086.

43. Panigrahy, D., M. L. Edin, C. R. Lee, S. Huang, D. R. Bielenberg, C. E. Butterfield, C. M. Barnes, A. Mammoto, T. Mammoto, A. Luria, et al. 2012. Epoxyeicosanoids stimulate multiorgan metastasis and tumor dormancy escape in mice. *J. Clin. Invest.* **122:** 178–191.

44. Fleming, I. 2007. Epoxyeicosatrienoic acids, cell signaling and angiogenesis. *Prostaglandins Other Lipid Mediat.* **82:** 60–67.

45. Frömel, T., B. Jungblut, J. Hu, C. Trouvain, E. Barbosa-Sicard, R. Popp, S. Liebner, S. Dimmeler, B. D. Hammock, and I. Fleming. 2012. Soluble epoxide hydrolase regulates hematopoietic progenitor cell function via generation of fatty acid diols. *Proc. Natl. Acad. Sci. USA.* **109:** 9995–10000.

46. Thompson, J. D., D. G. Higgins, and T. J. Gibson. 1994. CLUSTAL W: improving the sensitivity of progressive multiple sequence alignment through sequence weighting, position-specific gap penalties and weight matrix choice. *Nucleic Acids Res.* **22:** 4673–4680.